Electronic Supplementary Material (ESI) for Physical Chemistry Chemical Physics.


# Supplementary Information

## Two-step synthesis and characterizations of vertically stacked SnS-$WS_2$ and and SnS-$MoS_2$ p-n heterojunctions

Adha Sukma Aji,[a] Masanori Izumoto,[a] Kenshiro Suenaga,[a] Keisuke Yamamoto,[a] Hiroshi Nakashima,[ab] and Hiroki Ago*[ab]

[a]*Interdiscriplinary Graduate School of Engineering Sciences, Kyushu University, Fukuoka 816-8580, Japan*

[b]*Global Innovation Center (GIC), Kyushu University, Fukuoka 816-8580, Japan*

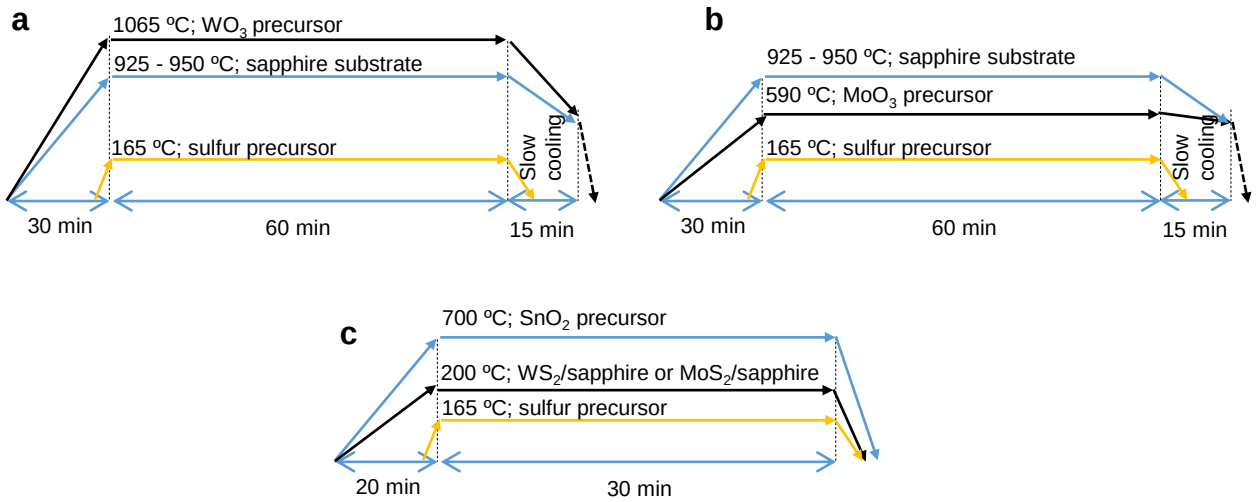


**Figure S1**. Temperature profiles of the first step CVD: (a) $WS_2$ and (b) $MoS_2$. (c) Temperature profile of the second CVD step used for the SnS growth.

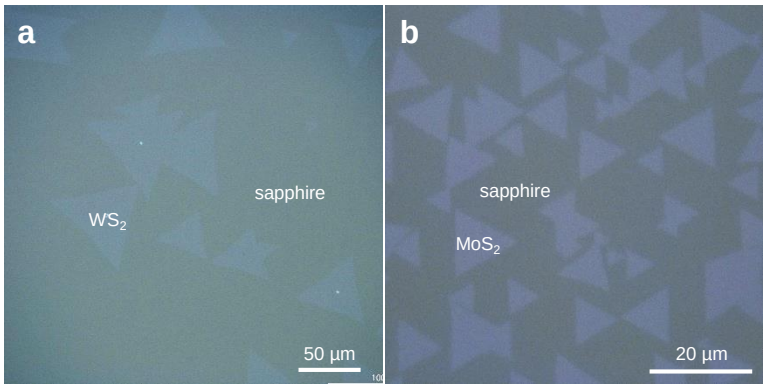


**Figure S2**. Optical microscope images of as-grown $WS_2$ (a) and $MoS_2$ (b) on sapphire substrates.

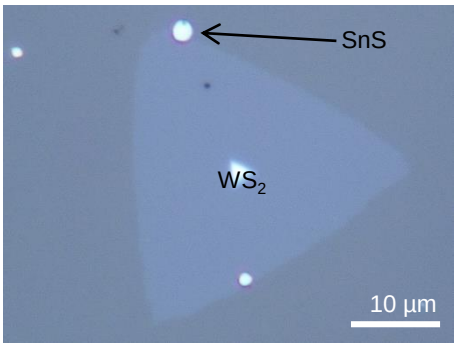


**Figure S3**. Optical microscope image of as-grown SnS-$WS_2$ at a low growth temperature (175 °C).

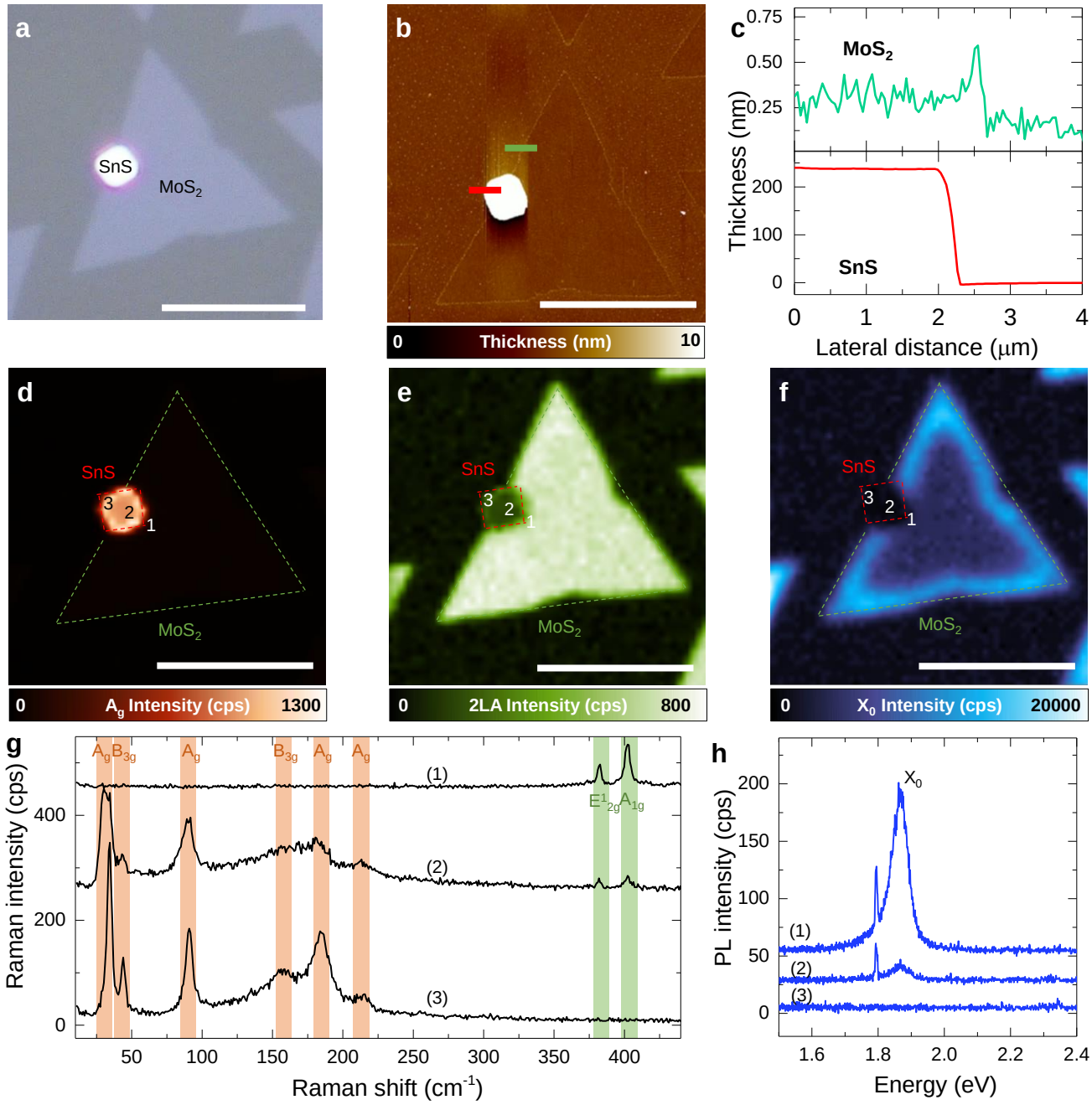


**Figure S4**. (a) Optical micrograph of a SnS-$MoS_2$ heterostructure. (b,c) AFM image and line profile of the SnS-$MoS_2$ heterostructure. (d,e) Raman intensity maps of $A_g$ peak of SnS and $E^1_{2g}$ peak of $MoS_2$. (f) PL intensity map of $MoS_2$. (g,h) Raman and PL spectra from the three points marked in (d)-(f). Red and green shaded areas indicate the Raman peaks from SnS and $MoS_2$, respectively. All scale bars are 10 μm.

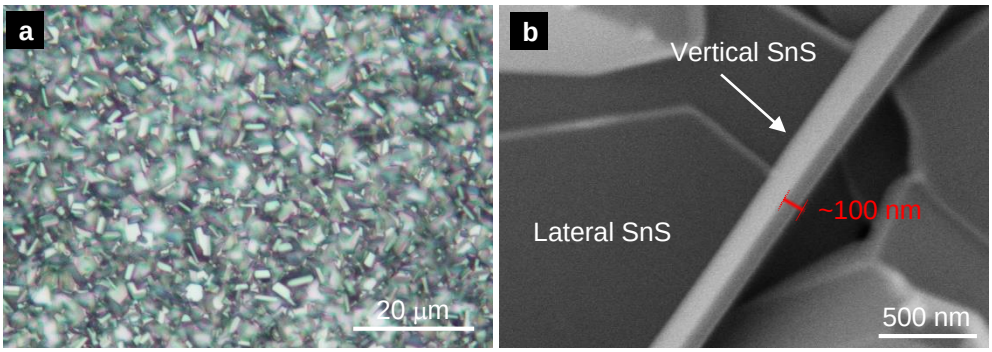


**Figure S5**. a) Optical micrograph and (b) SEM image of the product obtained by the low-pressure CVD growth of SnS at ~400 Pa. The pre-existing $WS_2$ grains are fully covered with SnS so that only SnS grains are observed on the substrate surface. The SnS grains grew both in lateral and vertical directions. The thickness of the vertically-grown SnS is about 100 nm (b).

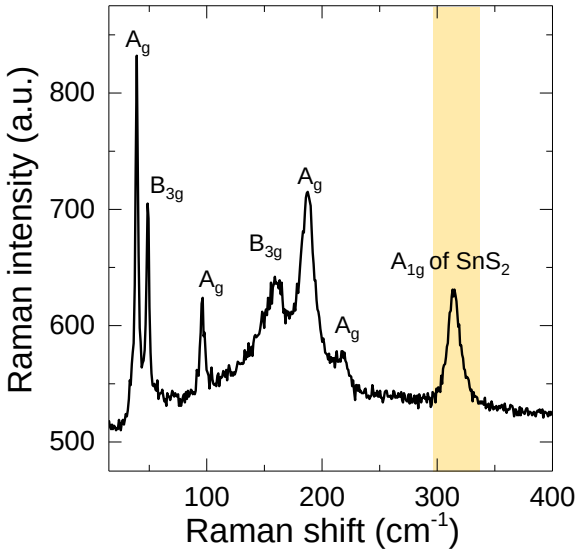


**Figure S6**. Raman spectrum of a SnS grain grown without $H_2$ gas flow during the CVD. The $A_{1g}$ peak from $SnS_2$ was detected in addition to the multiple peaks originated in SnS.

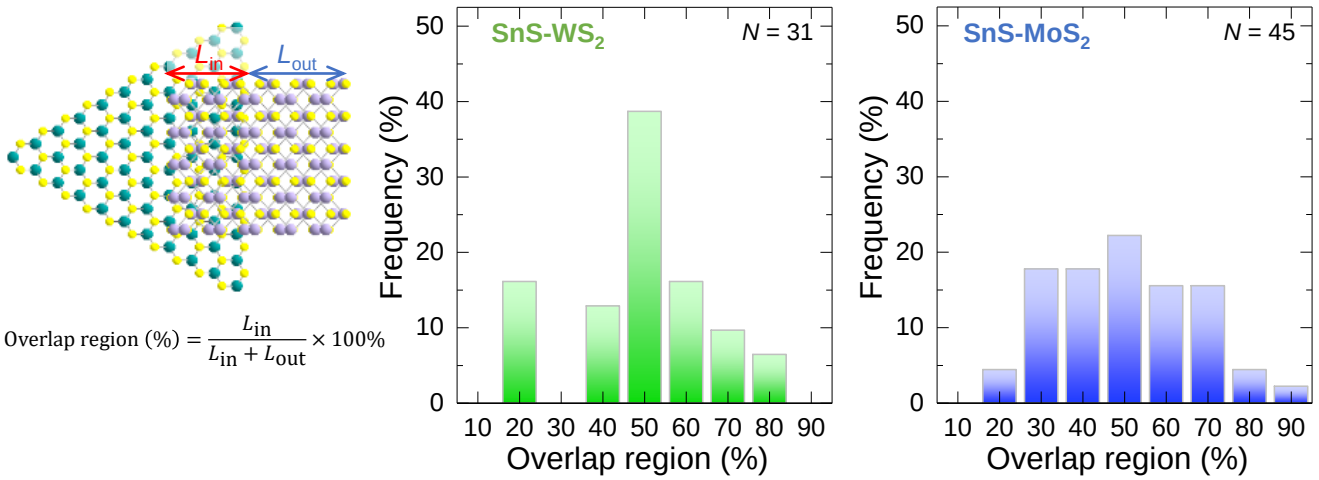


**Figure S7**. (a) Overlap region of SnS on $WS_2$ or $MoS_2$. Distribution of the overlap region in (b) SnS-$WS_2$ and (c) SnS-$MoS_2$ heterostructures.

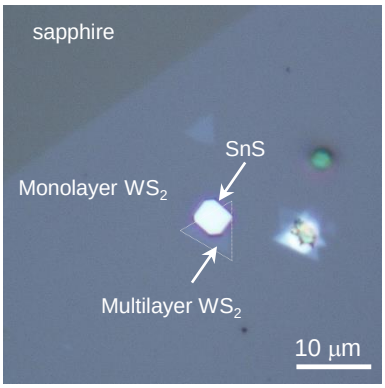


**Figure S8**. Optical microscope image of a large monolayer $WS_2$ grain with a SnS grain on the top. It is seen that SnS grows at the edge of the small multilayer $WS_2$ grain.

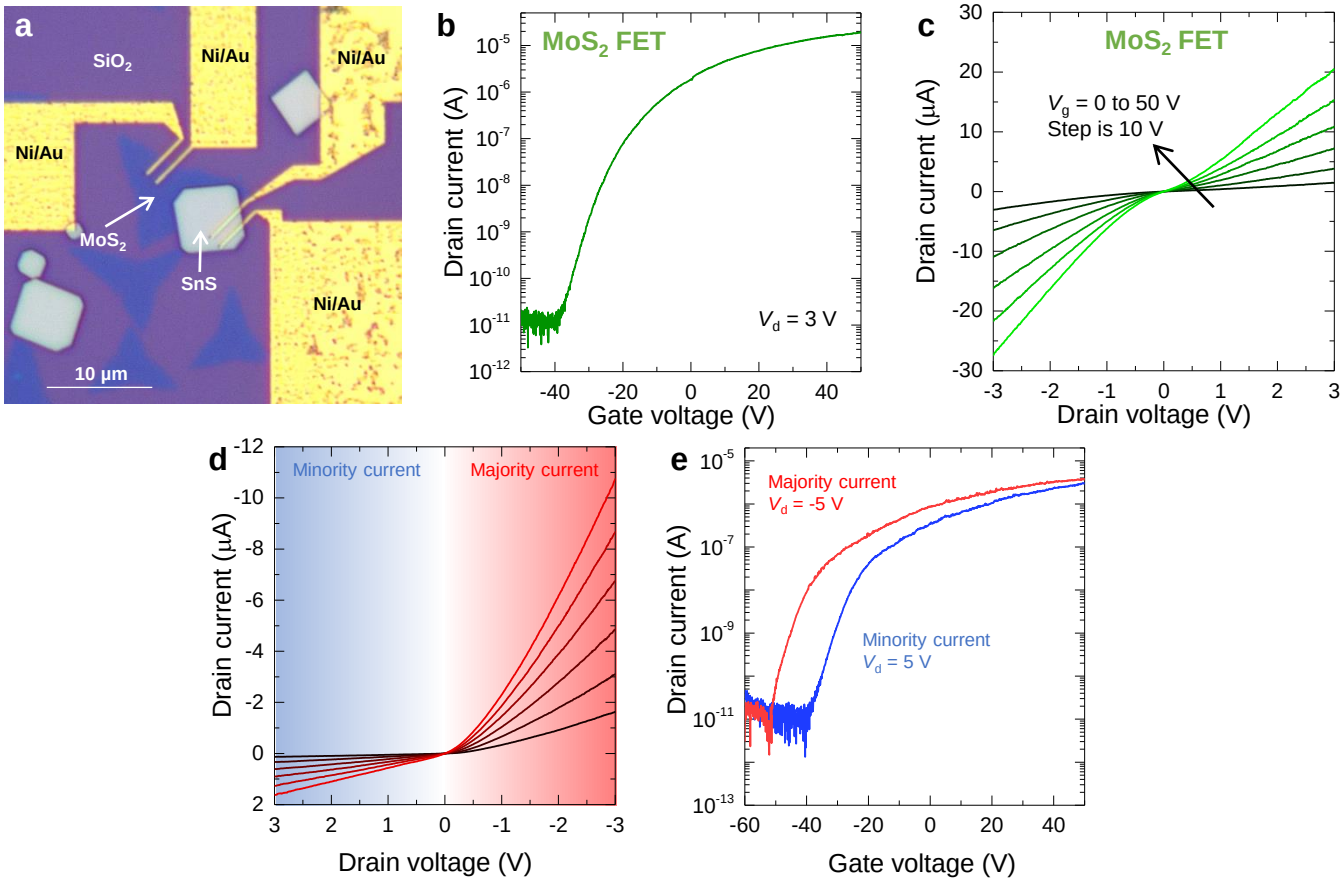


**Figure S9**. (a) Optical micrograph of the SnS-$MoS_2$ heterostructure FET. Transfer (b) and output (c) curves of $MoS_2$ FET. (d) Output curves of the SnS-$MoS_2$ heterostructure. (e) Transfer curves of the majority (red) and minority (blue) currents of the SnS-$MoS_2$ heterostructure.

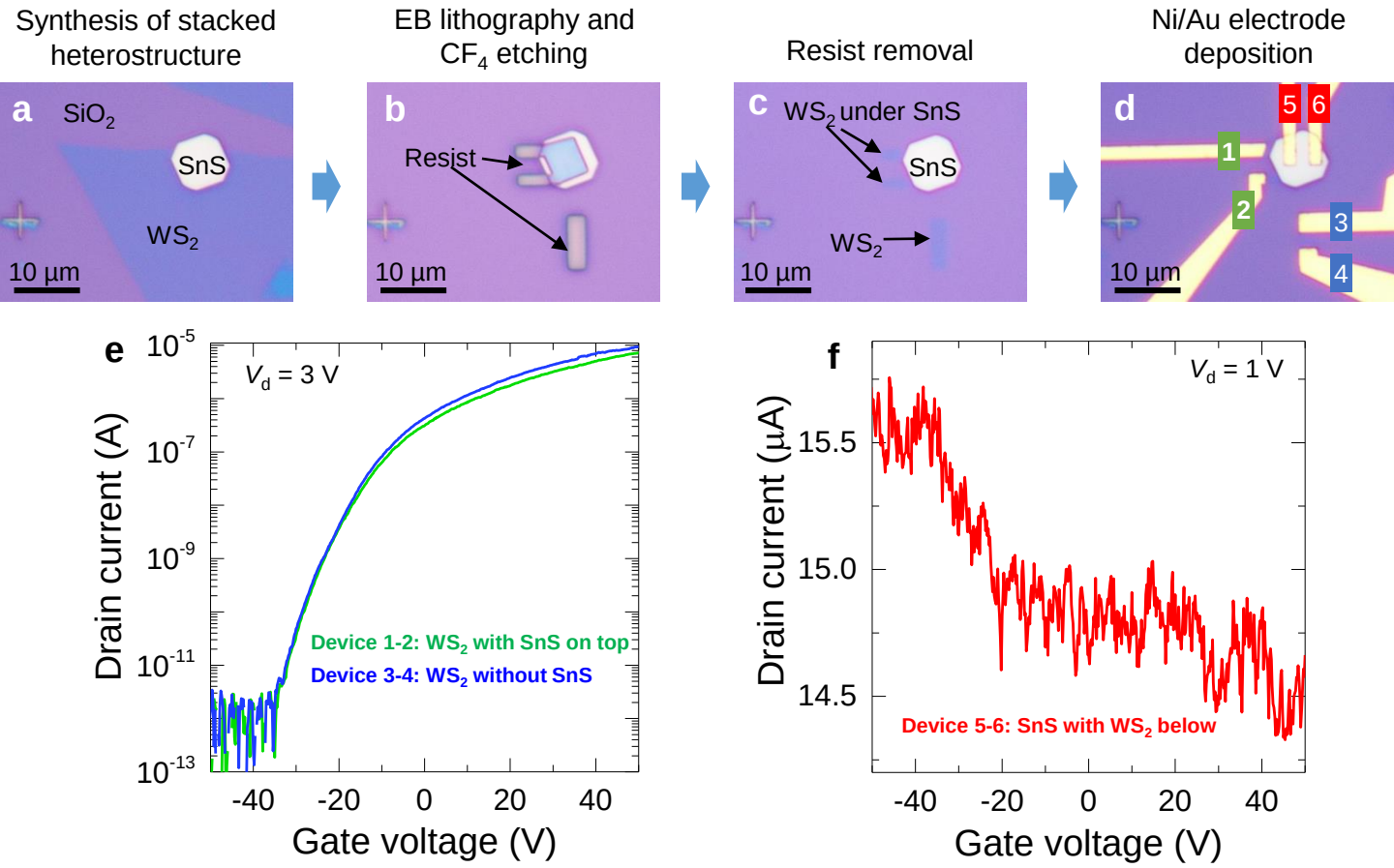


**Figure S10**. (a-d) Fabrication process of the $WS_2$ device with SnS on top and that without SnS. For comparison SnS device with $WS_2$ below was also fabricated. The device 1-2 measures the transport property of $WS_2$ channel with SnS on top. The device 3-4 shows the transport of $WS_2$ without SnS on top. The device 5-6 shows the transport of SnS with $WS_2$ underneath. (e) Transfer curves of the devices 1-2 and 3-4. (d) Transfer curve of the device 5-6.

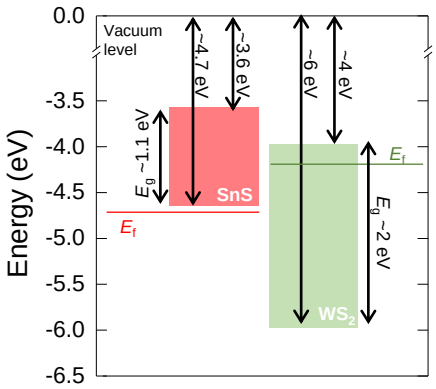


**Figure S11**. Band diagrams of SnS and $WS_2$. Red and green lines indicate the expected Fermi levels of SnS and $WS_2$, respectively. The band diagrams are taken from refs. 40 and 50.